ELSEVIER

Biochimica et Biophysica Acta 1324 (1997) 47–60

BIOCHIMICA ET BIOPHYSICA ACTA
BBA

Glycerol backbone conformation in phosphatidylcholines is primarily determined by the intramolecular stacking of the vicinally arranged acyl chains [1]

Ashish Arora, Chhitar M. Gupta *

Institute of Microbial Technology, Sector 39A, Chandigarh 160 036, India

Abstract

To analyse the effect of the altered glycerol backbone structure on the glycerophospholipid conformation, we have replaced the glycerol moiety by the *rac*-1,2,4-butanetriol residue in 1,2-diacyl-*sn*-glycero-3-phosphocholines (PC), and then analysed the resulting 1,2-dialkanoyloxy-*rac*-but-4-yl-[2-(trimethylammonium)ethyl] phosphates (1,2-bPC) and 1,3-dialkanoyloxy-*rac*-but-4-yl-[2-(trimethylammonium)ethyl] phosphates (1,3-bPC) by high-resolution ^{1}H- and ^{13}C-NMR spectroscopy in both $CDCl_3$ and D_2O. The preferred conformation about the C1–C2 glycerol bond in PC was almost completely preserved in 1,2-bPC, but it was completely random in case of 1,3-bPC. Out of the three C–C bonds present in the butanetriol backbone of 1,3-bPC, only the C2–C3 bond experienced a restricted rotation. However, the conformational preference about this bond was virtually similar to that observed for the C1–C2 bond in PC. These results clearly demonstrate that the preferred conformation of the glycerol backbone is determined primarily by the intramolecular acyl chain stacking which essentially requires a vicinal arrangement of the acyl chains in glycerophospholipids.

Keywords: Phospholipid conformation; Glycerol backbone; Butanetriol analog; NMR; Micelle; Bilayer

1. Introduction

Phospholipids are the major constituents of biological membranes, which provide the basic membrane matrix to which specific types of proteins and glycoproteins attach to form the functional membrane structure. Amongst the various classes of phospholipids present in animal cells, glycerophospholipids constitute the major portion [1]. This class of phospholipids primarily contain glycerol as their basic backbone to which three substituent chains are linked. The first two carbon atoms contain the two fatty acyl chains while the third carbon is linked to a free or monoesterified phosphate residue which is commonly termed as the polar head-group. These compounds due to their amphipathic character have a general tendency to form aggregates in an aqueous environment, and mainly exist in a bilayer configuration in biological membranes [2].

A number of studies have been performed to deter-

Abbreviations: NMR, nuclear magnetic resonance; DQF, double quantum filtered; NOE, nuclear Overhauser enhancement; TPPI, time proportion phase increment; COSY, correlated spectroscopy; NOESY, nuclear Overhauser enhancement spectroscopy; FT, Fourier transform; DCC, dicyclohexylcarbodiimide; DMAP, *N*,*N*-dimethyl-4-aminopyridine; TLC, thin-layer chromatography; IR, infrared; FAB, fast atom bombardment; LPPC, 1-lauroyl-propanediol-3-phosphorylcholine; T_m, main thermal transition temperature.

* Corresponding author. Fax: +91 172 690585 and 690632; E-mail: mg@imtech.ernet.in

[1] Communication No. 028/95 from I.M.T., Chandigarh, India.

PII S0005-2736

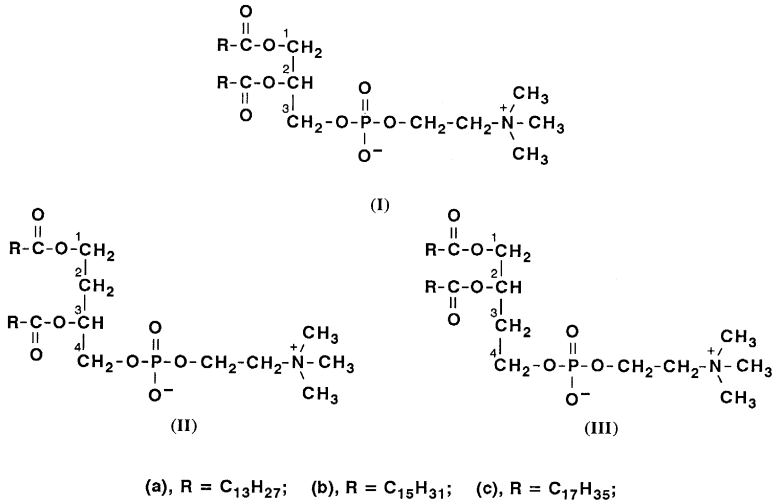

Fig. 1. Molecular structures of phosphatidylcholine analogs wherein the glycerol moiety has been replaced by the butanetriol residue.

mine the structure and dynamics of membrane phospholipids to understand their functional and structural roles in biomembranes. These molecules in crystals, aggregated form or solution have a preferred conformation which seems to be determined primarily by the glycerol backbone [3–5]. Although several investigators have studied the effect of the acyl chain and polar head-group modifications on the preferred conformations of the glycerol backbone [6–10], not much efforts have been made to analyse the effect of the altered glycerol structure on the backbone conformation. Here, we report the synthesis and high-resolution NMR characterization in $CDCl_3$ as well as in D_2O of the phosphatidylcholine analogs that have the butanetriol residue, instead of the glycerol moiety, as their backbone and the two acyl chains in 1,2- and 1,3-configurations (Fig. 1, II and III). Results of these studies demonstrate that the preferred conformation(s) of the glycerol backbone is determined mainly by the intramolecular acyl chain stacking which essentially requires a vicinal arrangement of these chains in glycerophospholipids.

2. Materials and methods

2.1. Materials

All the chemicals and solvents used in the synthesis were of the highest purity available. *rac*-1,2,4-Butanetriol was from Aldrich. Dicyclohexyl carbodiimide (DCC), *N*,*N*-dimethyl-4-aminopyridine (DMAP), stearic acid, palmitic acid, myristic acid, diisopropylethylamine, trimethylammonium chloride and Sephadex LH-20 were from Sigma. Benzylchloride, 10% Pd-C and silica gel (60–120 mesh) were from Sisco, Bombay. Tritylchloride and borontrifluoride-etherate were from Spectrochem, Bombay, and Fluka, Switzerland, respectively. 2-Chloro-2-oxo-1,3,2-dioxaphospholane was prepared by reacting ethyleneglycol with phosphorus trichloride [11] followed by oxidation of the reaction product with oxygen [12]. *N*-Triphenylmethyl-*N′*,*N′*-dimethyl-4-aminopyridinium chloride was prepared by reacting tritylchloride with DMAP in dichloromethane [13].

2.2. General methods

Purity of various reaction intermediates was checked by thin-layer chromatography (TLC) on silica gel G-60 plates. Homogeneity of phospholipids was established by both TLC and high-pressure liquid chromatography (HPLC). TLC plates were developed in chloroform/methanol/water (65:25:4, v/v/v) mixture and the phospholipids spots were visualized by staining the plate with iodine vapor followed by molybdenum-blue spray [14]. HPLC was performed using Waters HPLC pump (Model 510) along with Waters R 401 differential refractometer interfaced with Waters System Interface Module.

Chromatogrammes were analysed by using baseline 810 software. Analytical HPLC was performed on an Altex Ultrasphere C18 reverse-phase column (4.6 × 250 mm, particle size 5 μm) using ethanol/water/hexane (78:13:9, v/v/v) containing 25 mM cholinechloride at a flow rate of 0.5 ml/min as the elution system, whereas the preparative HPLC was carried out on an LKB TSK-ODS-120T semiprep column (7.8 × 300 mm, particle size 10 μm) using methanol/chloroform/water (90:10:4, v/v/v) at a flow rate of 2 ml/min as the eluent.

Phospholipids were purified by silica gel column chromatography, Sephadex LH-20 column (2.5 × 100 cm) chromatography, and preparative HPLC. The Sephadex LH-20 column was eluted with chloroform/methanol (1:1, v/v) mixture at a flow rate of about 60 ml/h. All the phospholipids thus-purified exhibited single spots on TLC and single peaks on analytical HPLC. While final phospholipids samples were characterized by high-resolution NMR analysis on a Bruker AM 500 FT NMR spectrometer and mass spectrometry, the intermediates were routinely characterized by NMR analysis on a Bruker WM-400 FT NMR spectrometer and infrared (IR) spectroscopy. IR spectra were recorded in KBr on a Perkin-Elmer 557 Grating spectrometer. Positive ion fast atom bombardment (FAB) mass spectrometry was performed on a Jeol JMS-SX 102 FAB mass spectrometer equipped with JMA-DA 6000 data system.

2.3. Preparation of NMR samples in organic solvent

Homogeneous phospholipid samples were azeotropically distilled several times with benzene and dried in vacuo at least for 4 h. The dry phospholipid powder thus-obtained is known to have 1–2 water molecules per phospholipid molecule [15]. The phospholipid samples were separately dissolved in $CDCl_3$ (99.8 atom% D; Sigma), and the solution was filtered, to give 30 mM final lipid concentration. The resulting phospholipid reverse micelles [16] were directly analysed by NMR spectroscopy.

2.4. Preparation of NMR samples in D_2O

Phospholipid solution in chloroform was evaporated to dryness under a slow jet of N_2 giving rise to the formation of a thin lipid film on the walls of the tube. Final traces of the solvent were removed by leaving the tube in vacuo for 3–4 h. The dried lipid mixture was dispersed in D_2O (99.996 atom % D; Sigma) at 50°C. The mixture was first vortexed for 15 min at 50°C and then sonicated (50°C) for 40 min under N_2 using a probe-type sonicator (Heat Systems Ultrasonic Processor XL) at 15% power setting. The sonicated mixture was centrifuged at 107 000 × g for 60 min at 25°C to remove titanium particles as well as poorly dispersed lipids. Only the top two-thirds of the supernatant was used in the NMR experiment. The size of the phospholipid vesicles thus-obtained was determined by both the negative-staining electron microscopy and laser light scattering. The mean outer diameter of these vesicles was about 26 nm.

2.5. NMR spectroscopy in $CDCl_3$

High-resolution ^1H- and ^{13}C-NMR spectra of phospholipids were recorded on a Bruker AM 500 FT-NMR spectrometer operating at 500 MHz for ^1H and 125.8 MHz for ^{13}C, with a digital resolution of 0.08 Hz/point for ^1H and 1.66 Hz/point for ^{13}C, for one-dimensional spectra. All the experiments were carried out at 25°C. Two-dimensional $^1H-^1H$-double quantum filtered (DQF) correlated spectra and nuclear Overhauser enhancement (NOE) spectra were recorded in the phase sensitive mode using time proportion phase increment method (TPPI). 512 T_1 increments of 2048 complex points were acquired and then zero-filled to 2048 × 1024 matrix for DQF-correlated spectroscopy (DQF-COSY) and 1024 × 512 matrix for NOE spectroscopy (NOESY). 64 scans were recorded for DQF-COSY, whereas for NOESY the number of scans was 32. Shifted sine-bell apodization of $\pi/8$ in F_2 and $\pi/2$ in F_1 was used prior to double fourier transformation. A mixing time of 300 ms was used for the NOESY.

The $^1H-^{13}C$-correlated spectra were recorded on a Bruker ACP 300 FT-NMR spectrometer operating at 300 MHz in the normal mode.

The chemical shifts and coupling constants of the resonances from the protons of phospholipid backbone were obtained from computer simulations of experimental spectra using the program LAOCUN on an IRIS 4D/70G work station. The accuracy of the

spin–spin coupling constants derived from the spectral simulation was 0.1 Hz. The fractional populations of the major conformational rotamers were calculated from the observed vicinal spin-coupling constants, by using a generalized Karplus equation [17,18] on the basis of the assumption that the observed coupling constants represented averages of the component coupling constants of each of the three staggered-state minimum energy conformers, which are weighted by their fractional populations.

2.6. NMR spectroscopy in D_2O

The ^{1}H-NMR spectra were recorded at 50°C on a Bruker ACP 300 FT-NMR spectrometer operating at 300 MHz and equipped with a 5 mm quadrupole nuclei probe and ASPECT 3000 computer, using DISNMR program version 900101.11. 4,4-Dimethyl-4-silapentane sodium sulfonate in D_2O was taken as the external reference, and water signals were suppressed by using PRESAT · AU pulse sequence. A pulse width of 16 μs (90°), and sweep width of 5000 Hz were used to record 32K data points, with an acquisition time of 1.638 s, and resolution of 0.305 Hz/point. The number of scans were 120–200 and a line broadening factor of 0.3 Hz was used.

The broad band ^{1}H-decoupled ^{13}C-NMR spectra were recorded at 75.4 MHz at 50°C, using composite pulse decoupling, with an accuracy of 0.01 ppm for chemical shifts. A pulse width of 6 μs (90°) and sweep width of 20 000 Hz were used to record 16K data points with an acquisition time of 0.205 s. A digital resolution of 2.44 Hz/point and a line broadening factor of 4 Hz was used. The number of scans were 10 000–12 000 [19].

2.7. Preparation of phospholipids

1,2-Diacyl-*sn*-glycero-3-phosphocholines (Ia–Ic, Fig. 1) were prepared by acylation of *sn*-glycero-3-phosphorylcholine with appropriate fatty acid anhydrides in the presence of DMAP [20]. 1,3-Difattyacyloxy-*rac*-but-4-yl-[2-(trimethylammonium)ethyl] phosphates (IIa–IIc, Fig. 1) and 1,2-difattyacyloxy-*rac*-but-4-yl-[2-(trimethylammonium)ethyl] phosphates (IIIa–IIIc, Fig. 1) were prepared from *rac*-1,2,4-butanetriol in several steps. A brief description of their synthesis is given below:

2.7.1. Preparation of 1,3-dihexadecanoyloxy-rac-but-4-yl-[2-(trimethylammonium)ethyl] phosphate (IIb)

Distilled *rac*-1,2,4-butanetriol (IV) (10.6 g, 0.1 mol) and benzaldehyde (25.4 ml, 0.25 mol) were treated with 10% HCl (100 μl) in anhydrous methanol. The mixture was stirred vigorously for 1 h at room temperature (about 25°C) followed by 15 min at 45–50°C under vacuo (4 mm). The reaction mixture was cooled, and to it was added chloroform (100 ml). The resulting solution was washed with 5% $NaHCO_3$ (2×50 ml) followed with water (3×50 ml). The organic layer was dried over anhydrous sodium sulfate. The solvent was removed and the residue subjected to fractional distillation under vacuo to afford 4-hydroxymethyl-1,3-(2-phenyl)dioxane (V). It was further purified by chromatography over silica gel column (1.8×100 cm) using benzene/ethylacetate mixture as the eluent. The pure V was eluted in benzene containing 3% ethylacetate. The purity was checked by TLC using benzene/chloroform/ethylacetate/methanol (60:20:4:1, v/v) as the solvent system. Yield: 11.2–12.0 g (57–62%). ^{1}H-NMR ($CDCl_3$) δ 7.50–7.30 (m, 5H, C_6H_5), 5.47 (s, 1H, C*H*–C_6H_5), 4.25–4.20 (m, 1H, O–C*H*), 3.93–3.85 (m, 2H, O–CH_2), 3.65–3.55 (m, 2H, CH_2OH), 1.88–1.74 (m, 1H, CH_2–CH_AH$_B$–CH), 1.38–1.32 (m, 1H, CH_2–$CH_A H_B$–CH).

Compound V (20 g, 103 mmol) was converted into 4-benzyloxymethyl-1,3-(2-phenyl)dioxane (VI) by reacting it with benzyl chloride (freshly distilled, 13.05 ml; 100 mmol) and powdered KOH (87 g, 1.55 mol) in presence of DMAP (100 mg) in anhydrous benzene (400 ml), as described earlier [21]. The product was purified by fractional distillation. Yield: 20 g (83%); b.p. 173°C at 0.8 mm; m/z 284 (M^+); ^{1}H-NMR ($CDCl_3$) δ 7.60–7.20 (m, 10H, C_6H_5), 5.53 (s, 1H, C*H*–C_6H_5), 4.64–4.55 (m, 2H, CH_2–C_6H_5), 4.31–4.25 (m, 1H, O–C*H*), 4.18–4.16 (m, 1H, CH_AH$_B$-O), 4.02–3.93 (dt, $J = 11.90$ Hz and 2.60 Hz, 1H, $CH_A H_B$-O), 3.69–3.64 (dd, $J = 10.20$ Hz and 6.00 Hz, 1H, CH_AH$_B$-$OCH_2C_6H_5$), 3.55–3.50 (dd, $J = 10.20$ and 4.80 Hz, 1H, $CH_A H_B$-$OCH_2C_6H_5$), 1.95–1.80 (m, 1H, CH_2–CH_AH$_B$–CH), 1.62–1.54 (m, 1H, $CH_2CH_A H_B$–CH).

Compound VI (5 g, 176 mmol) was treated with aqueous HCl (0.01 N, 150 ml) at 120–130°C for 6 h. The reaction mixture after cooling was neutralized with aqueous $NaHCO_3$ solution (5%) saturated with NaCl. It was extracted several times with chloroform (50 ml × 6). The organic phase was dried over anhydrous sodium sulfate and the solvent was removed. The residue thus-obtained was run over a silica gel column using chloroform/benzene mixture as the eluent. 4-Benzyloxy-1,3-dihydroxy-*rac*-butane (VII) was eluted in chloroform containing 30% (v/v) benzene. Yield: 2.3 g (70%); m.p. 74–77°C; *m/z* 196 (M^+); ^{1}H-NMR ($CDCl_3$) δ 7.45–7.25 (m,5H, C_6H_5), 4.54 (s, 2H, CH_2–C_6H_5), 4.12–4.04 (m, 1H, C*H*-O), 3.85–3.76 (t, $J = 5.50$ Hz, 2H, CH_2-OH), 3.55–3.48 (dd, $J = 9.40$ Hz and 3.50 Hz, 1H, CH_AH_B-$OCH_2C_6H_5$), 3.44–3.36 (dd, $J = 9.40$ Hz and 7.50 Hz, 1H, CH_AH_B-$OCH_2C_6H_5$), 1.88–1.65 (m, 2H, CH_2–CH_2–CH).

Compound VII (1.0 g, 5 mmol) was converted into 1,3-dihexadecanoyloxy-4-benzyloxy-*rac*-butane (VIII) by reacting it with palmitic anhydride (5.6 g, 11 mmol) in presence of DMAP (1.25 g, 10 mmol) in anhydrous chloroform (100 ml) as reported earlier [20]. Pure VIII was isolated by chromatography first over silica gel using ethylacetate/n-hexane as the eluent, and then over Sephadex LH-20. Yield: 2.8 g (80%); m.p. 38–40°C. IR (KBr) ν_{max} cm^{-1} 1760 (C=O); ^{1}H-NMR ($CDCl_3$) δ 7.45–7.30 (m, 5H, C_6H_5), 5.34–5.26 (m, 1H, C*H*-O), 4.64–4.50 (m, 2H, CH_2–C_6H_5), 4.20–4.10 (m, 2H, CH_2-O), 3.60–3.52 (m, 2H, CH_2-O).

A solution of VIII (2 g, 3 mmol) in ethanol/ethylacetate (85:15, v/v) mixture (40 ml) was hydrogenated over Pd-C (10%, 700 mg) at room temperature at 60 psi for 12 h. The catalyst was removed and the solvent evaporated off under vacuo. The residue was purified by chromatography over Sephadex LH-20 column to give 1,3-dihexadecanoyloxy-4-hydroxy-*rac*-butane (IX). Yield: 1.6 g (90%); m.p. 73–75°C; IR (KBr) ν_{max} cm^{-1} 3300 (OH) and 1740 (C=O); *m/z* 564 (M^+-H_2O); NMR ($CDCl_3$) δ 5.10–5.00 (m, 1H, C*H*-O), 4.24–4.10 (m, 2H,CH_2–O), 3.80–3.60 (m, 2H, CH_2–OH).

The phosphocholine residue was introduced in IX following the published procedure [22]. Pure IIb was isolated by chromatography over silica gel and Sephadex LH-20, and finally by HPLC. Yield: 93 mg (65%); IR (KBr) ν_{max} cm^{-1} 3430 (OH), 1735 (C=O), 1630 {N^+ $(CH_3)_3$}, 1240 (P=O), 1090 (P=O); FAB Mass 749 (MH^+). Compounds IIa and IIc were similarly prepared, purified and characterized.

2.7.2. Preparation of 1,2-dihexadecanoyloxy-rac-but-4-yl-[2-(trimethylammonium)ethyl] phosphate (IIIb)

Phospholipids IIIa–IIIc were prepared from compound V. Compound V (4.85 g, 25 mmol) was converted into 4-hexadecanoyloxymethyl-1,3-(2-phenyl)dioxane (X) by reacting it with palmitic anhydride (14.92 g, 30 mmol) in presence of DMAP (3.35 g, 27.5 mmol) in dry chloroform (200 ml), as described earlier [20]. The crude material was chromatographed over silica gel column (1.8 cm × 100 cm) using ethylacetate/n-hexane as the eluant. Pure X was eluted in hexane containing 2% ethylacetate. Yield: 9.5 g (88%); m.p. 60–62°C; IR (KBr) ν_{max} cm^{-1} 1750 (C=O) and 1080 (C–O–C); ^{1}H-NMR ($CDCl_3$) δ 7.50–7.30 (m, 5H, C_6H_5), 5.55 (s, 1H, C*H*–C_6H_5), 4.38–4.28 (m, 1H, C*H*-O), 4.25–4.10 (m, 3H, CH_2-O and CH_AH_B–O), 4.05–3.95 (m, 1H, CH_AH_B-O).

A solution of X (5 g, 11.6 mmol) in ethanol/ethylacetate (85:15, v/v) mixture (100 ml) was hydrogenated over Pd-C (10%; 2 g) at room temperature for 24 h at 60 psi. The catalyst was removed by filtration. The residue obtained after removing the solvent was chromatographed over a silica gel column (1.2 × 30 cm) using methanol/chloroform as the eluent. Pure 1-hexadecanoyloxy-2,4-dihydroxy-*rac*-butane (XI) was eluted in chloroform containing 1.5% methanol. Yield: 3.2–3.4 g (80–85%); m.p. 55–58°C; IR (KBr) ν_{max} cm^{-1} 3300 (OH) and 1740 (C=O); ^{1}H-NMR ($CDCl_3$) δ 4.20–4.00 (m, 3H, C*H*–O and CH_2–O), 3.95–3.85 (m, 2H, CH_2–O).

Compound XI (2 g, 6 mmol) was tritylated by reacting it with 1-trityl-*N*,*N*-dimethyl-4-aminopyridinium chloride (2.58 g, 6.6 mmol) in anhydrous dichloromethane (60 ml) as described earlier [13]. The crude material was chromatographed first over silica gel using benzene as the eluent and then over Sephadex LH-20 to give pure oily 1-hexadecanoyloxy-2-hydroxy-4-trityloxy-*rac*-butane (XII). Yield: 2.4 g (70%). IR (Neat) ν_{max} cm^{-1} 1750 (C=O); ^{1}H NMR ($CDCl_3$) δ 7.50–7.00 (m, 15H, C_6H_5), 4.10–3.95 (m, 3H, C*H*–O and CH_2-O),

3.48–3.42 (m, 1H, CH_AH$_B$–O), 3.34–3.24 (m, 1H, CH$_A$$H_B$–O).

Compound XII (1.0 g, 1.7 mmol) was converted into 1,2-dihexadecanoyloxy-4-trityloxy-*rac*-butane (XIII) by reacting it with palmitic anhydride (0.92 g, 1.9 mmol) in presence of DMAP (208 mg, 1.7 mmol) in anhydrous chloroform (60 ml) according to Gupta et al. [20]. The desired product XIII was isolated in pure form after chromatography over silica gel using benzene/n-hexane as the eluent. Yield: 1.27 g (90%); m.p. 60–62°C; IR (KBr) ν_{max} cm^{-1} 1740 (C=O); ^{1}H-NMR (CDCl$_3$) δ 7.50–7.20 (m, 15H, C$_6$$H_5$), 5.28 (m, 1H, C$H$–O), 4.30–4.24 (dd, J = 11.90 Hz and 3.10 Hz, 1H, CH_AH$_B$–O), 4.05–4.00 (dd, J = 11.90 Hz and 6.25 Hz, 1H, CH$_A$$H_B$–O), 3.10–3.00 (t, J = 6.20 Hz, 2H, CH_2–O).

To a chilled solution of XIII (300 mg, 0.364 mmol) in anhydrous dichloromethane (25 ml) was added freshly distilled borontrifluoride-etherate (25 μl, 1.2 mmol). The solution was stirred at 5°C for 2h. After completion of the reaction, a solution of saturated NaHCO$_3$ (15 ml) was added and the mixture further stirred for another 15 min. The dichloromethane layer was separated and washed with aqueous NaHCO$_3$ solution (5%; 10 ml × 2) and water (10 ml × 3), and dried over anhydrous sodium sulfate. The solvent was removed and the residue chromatographed over Sephadex LH-20 column to afford pure 1,2-dihexadecanoyloxy-4-hydroxy-*rac*-butane (XIV). Yield: 170 mg (80%); m.p. 60–62°C. IR (KBr) ν_{max} cm^{-1} 3300 (OH) and 1740 (C=O); ^{1}H NMR (CDCl$_3$) δ 5.30– 5.24 (m, 1H, CH-O), 4.26–4.20 (dd, J = 11.30 Hz and 3.10 Hz, 1H, CH_AH$_B$-O), 4.16–4.10 (dd, J = 11.30 and 6.25 Hz, 1H, CH$_A$$H_B$-O), 3.74–3.66 (m, 1H, C$H_AH_B$-OH), 3.60–3.52 (m, 1H, CH$_A$$H_B$-OH).

The phosphocholine residue was introduced in XIV, essentially as described in preparation of IIb, to yield IIIb. FAB Mass 749 (MH$^+$). Compounds IIIa and IIIc were similarly prepared, purified and characterized.

3. Results

The structural changes that were introduced in the glycerol backbone were based on the consideration that the introduction of an additional methylene residue between the C1 and C2 carbon atoms in I would increase the intramolecular acyl chain distance and hence should enable us to analyse the role of acyl chain aggregation in determining the preferred conformation around the glycerol C1–C2 bond [6]. Similarly, the insertion of an extra methylene residue between the C2 and C3 carbon atoms in I should help us to analyse the influence, if any, of the polar head-group structure on the glycerol backbone con-

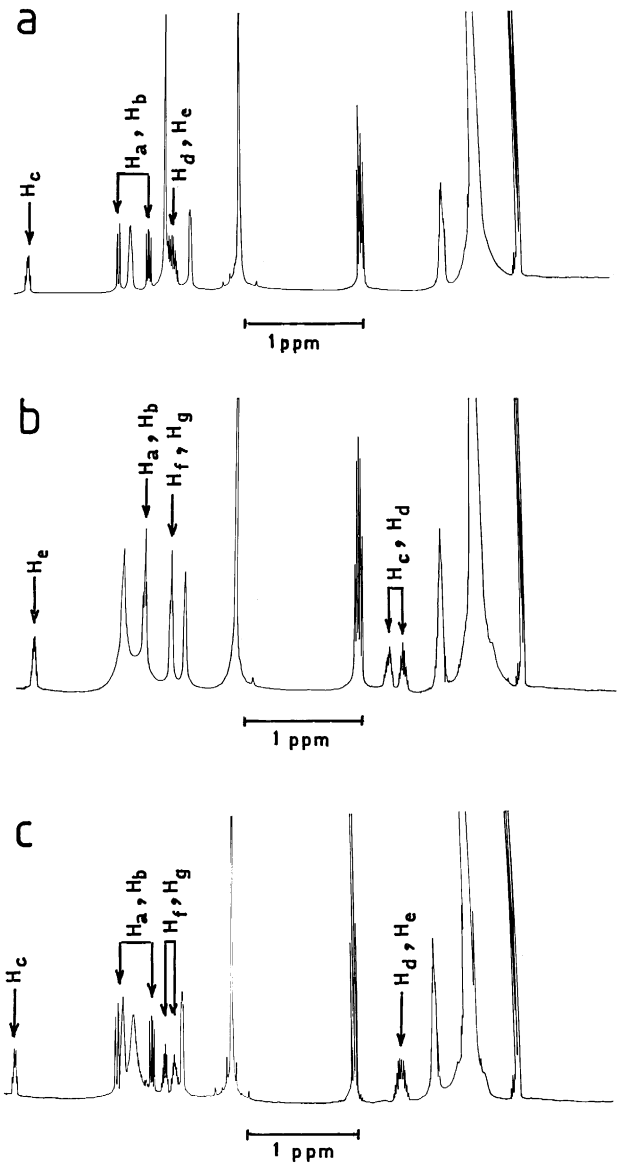

Fig. 2. 500 MHz ^{1}H NMR spectra of **Ib** (a), **IIb** (b), and **IIIb** (c). All the spectra were recorded by using 30 mM solutions of each phospholipid in CDCl$_3$ as described in Materials and Methods. For proton numbering: see Table 1.

formation. Besides, these changes could also prove useful in evaluating the uniqueness of the glycerol structure in serving as the backbone in majority of the membrane phospholipids.

Phosphatidylcholines (I) and their analogs II and III were synthesized and subsequently purified by silica gel and Sephadex LH-20 column chromatography, and HPLC prior to analysing their structures in $CDCl_3$ by 500 MHz high-resolution NMR spectroscopy. Peak assignments in the various phospholipid molecules were made from the homonuclear two-dimensional DQF-COSY in conjunction with the anticipated chemical shifts of each functional group. Proton-decoupled ^{13}C-NMR spectra were assigned on the basis of their correlation with the ^{1}H-NMR spectra by hetero COSY.

The typical ^{1}H-NMR spectra of the three representative phospholipid samples, viz. Ib, IIb and IIIb, in $CDCl_3$ are shown in Fig. 2. As may be seen in the figure, the ^{1}H-NMR of Ib (Fig. 2a) differed markedly from that of IIb and IIIb (Fig. 2b and c). This difference was limited not only to the differences in the chemical shifts but it could also be seen in splitting patterns of some peaks. The chemical shifts as well as the geminal and vicinal coupling constants of the various protons in the glycerol/butanetriol backbone of Ib, IIb and IIIb (from analysis of computer simulations of experimental spectra) are listed in Table 1, and the simulated spectra are shown in Fig. 3. The amount of water present in the various phospholipids samples in $CDCl_3$ was about 2–4 water molecules/phospholipid molecule, as judged from the water protons-to-phospholipid protons signals ratio.

The chemical shift difference between the two C1 methylene protons (H_a and H_b) in IIIb was the largest (0.308 ppm) as compared to Ib (0.268 ppm) and IIb (0 ppm), indicating that these protons in IIIb are more nonequivalent, compared to Ib. However, in case of IIb, these protons were both chemically and magnetically equivalent, which is similar to that reported earlier for 1-lauroylpropanediol-3-phosphorylcholine (LPPC) [23]. The C3 methylene protons in Ib and C4 methylene protons in IIb and IIIb were identified by irradiation of the vicinally coupled protons as well as on the basis of the ^{31}P-^{1}H couplings. These protons in Ib and IIIb were nonequivalent both chemically and magnetically, having geminal coupling constants of 11.0 Hz and 10.7 Hz, respectively. In contrast, no such nonequivalence was observed in case of IIb (Fig. 2b, H_f and H_g).

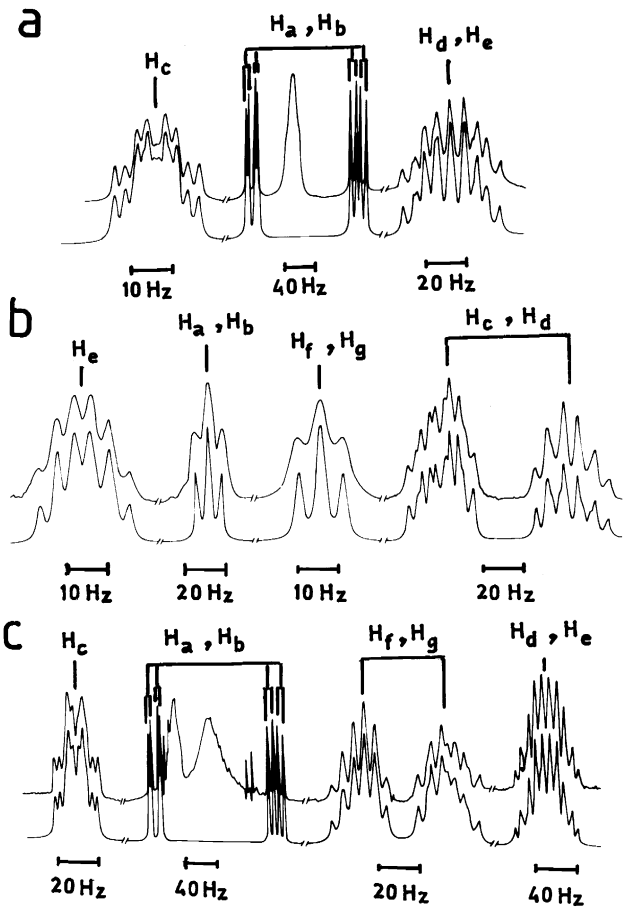

Fig. 3. Expanded experimental spectra (top) and computer simulations (bottom) of the glycerol/butanetriol backbone protons in **Ib** (a), **IIb** (b), and **IIIb** (c). For proton numbering: see Table 1.

The C2 methine proton in IIIb (or Ib) or C3 methine proton in IIb was identified by its distinct chemical shift. This proton in case of Ib appeared at 5.178 ppm, but it shifted upfield, as in IIb (5.051 ppm), or downfield, as in IIIb (5.223 ppm), by changing its relative disposition with respect to the C1 ester group or the phosphocholine residue, suggesting that the stereo-electronic environment of this proton is different in IIb and IIIb, as compared to Ib.

The C2 methylene protons in IIb were characterized after irradiating the C1 methylene protons, resulting in collapse of the complex spectra into an octet, representative of an ABX pattern, from which a geminal coupling of 14.4 Hz and vicinal couplings

Table 1
Chemical shifts and coupling constants of glycerol/butanetriol backbone protons in Ib, IIb and IIIb [a]

Molecular species	^{1}H chemical shift (ppm) [b]						
	a [c]	b	c	d	e	f	g
Ib	4.376	4.108	5.178	3.916	3.871	–	–
IIb	4.091	4.091	2.008	1.895	5.051	3.847	3.847
IIb	4.318	4.010	5.223	1.888	1.840	3.894	3.799

	Coupling constant (Hz) [d]															
	J_{ab}	J_{ac}	J_{ad}	J_{bc}	J_{bd}	J_{cd}	J_{ce}	J_{de}	J_{df}	J_{dg}	J_{ef}	J_{eg}	J_{fg}	J_{fp}	J_{gp}	J_{dp}	J_{ep}
Ib	12.03	7.22	–	2.86	–	5.80	5.40	11.00	–	–	–	–	–	–	–	7.20	7.10
IIb	0	6.20	5.60	6.80	6.00	14.40	8.20	4.00	–	–	5.20	5.20	0	6.10	6.10	–	–
IIIb	13.60	6.90	–	2.69	–	7.80	5.40	14.40	8.00	5.00	5.56	4.76	10.70	7.20	6.50	–	–

[a] All experiments were carried out in $CDCl_3$ at 25°C on a Bruker AM 500 FT-NMR spectrometer.
[b] Chemical shifts are expressed in parts per million down-field from tetramethylsilane. The accuracy of chemical shifts is ± 0.001 ppm.
[c] Protons in Ib, IIb and IIIb are labelled as follows:

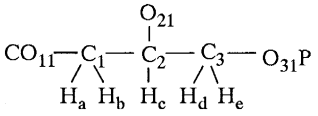

Ib

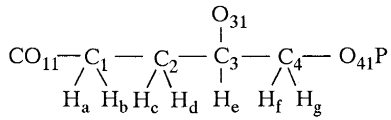

IIb

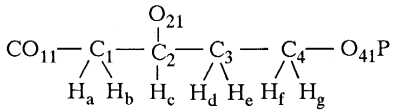

IIIb

[d] Coupling constants were obtained from computer simulations of experimental spectra. The accuracy of coupling constants is upto 0.1 Hz.

Table 2
^{13}C Chemical shifts of glycerol/butanetriol backbone and polar head group carbons in Ib, IIb and IIIb [a]

Molecular species	^{13}C chemical shifts (ppm) [b]					
	$\underline{CH_2}OCO$ [c]	$\underline{CH}OCO$	$\underline{CH_2}OP$	$PO\underline{CH_2}$	$N\underline{CH_2}$	$N\underline{CH_3}$
Ib	63.01	70.48	63.44	59.38	66.30	54.33
	(63.20) [d]	(70.87)	(63.89)	(59.66)	(66.34)	(54.34)
IIb	60.58	69.92	66.12	59.41	66.33	54.42
	(60.90)	(70.65)	(66.50)	(59.62)	(66.35)	(54.35)
IIIb	64.95	68.69	61.28	59.30	66.30	54.34
	(65.45)	(69.43)	(61.86)	(59.52)	(66.33)	(54.32)

[a] All experiments were carried out in $CDCl_3$ at 25°C on a Bruker AM 500 FT-NMR spectrometer.
[b] Chemical shifts are expressed in parts per million down field from tetramethylsilane. The accuracy of chemical shifts is ± 0.01 ppm.
[c] The chemical shift given is that of the C-atom underlined.
[d] Values shown in parantheses denote the chemical shifts of the respective carbon atoms in sonicated aqueous dispersions. These chemical shifts have been expressed in parts per million down field from 4,4-dimethyl-4-silapentane sodium sulfonate.

with C3 methine proton of 8.2 Hz and 4.0 Hz were obtained. These two protons, therefore, represented the AB part of an ABM_2X spectrum, and were both chemically and magnetically nonequivalent. In fact, this was the only methylene residue in IIb which bore nonequivalent protons. The remaining couplings of these protons with the C1 methylene protons were ascertained from the first order triplet spectrum of the C1 methylene protons. Similarly, for characterizing the C3 methylene protons in IIIb, the C4 methylene protons were irradiated, simplifying the complex spectrum to an octet from which a geminal coupling of 14.4 Hz and vicinal couplings with C2 methine proton of 7.8 Hz and 5.4 Hz were obtained. Thus, these protons in IIIb also, like the C2 methylene protons in IIb, were chemically and magnetically nonequivalent, albeit to a lesser extent.

These results indicate some degree of similarity between the structures of the glycerol backbone of Ib and the butanetriol backbone of IIIb. In both the cases, a high degree of conformational preference was observed around the C1–C2 and C2–C3 bonds. However, no such conformational preference was seen in IIb about the C1–C2 and C3–C4 bonds,

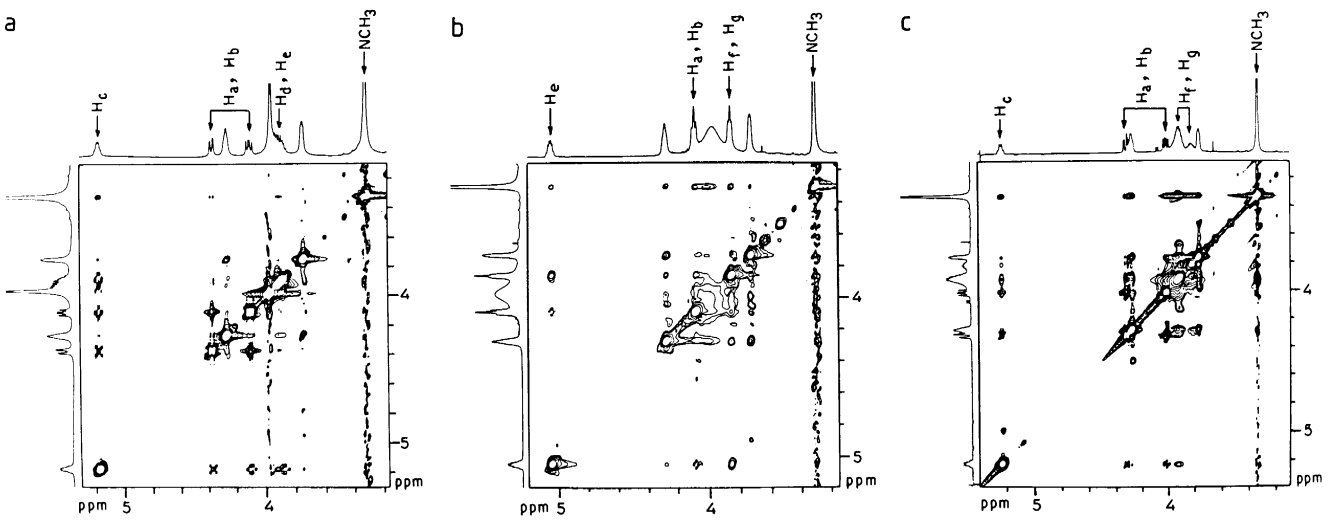

Fig. 4. Two-dimensional nuclear Overhauser enhancement spectra of Ib (a), IIb (b), and IIIb (c) in $CDCl_3$ using a mixing time of 300 ms. The spectra were recorded as described in Section 2. For proton numbering: see Table 1.

suggesting that the structure of this phospholipid molecule is quite flexible about these bonds which primarily determine the orientation of the C1 acyl chain and the phosphocholine residue with respect to the C3 acyl chain. Interestingly, the only methylene which bore nonequivalent protons in IIb was the C2 methylene that separated the two carbon atoms bearing the fatty acyl chains. This indicates some degree of conformational preference even in IIb about the C1–C2–C3 bond.

NMR and X-ray studies [3,10] have revealed that the preferred conformation of the phosphocholine head-group in phosphatidylcholines may be characterized by an almost exclusively gauche conformation of the choline group and predominantly *antiperiplanar* conformation about the C–C–O–P and P–O–C–C bonds. Since each of the three phospholipid molecular species examined in the present study have $^{31}P-^{1}H$ coupling constants [24] in the range of 6.1–7.2 Hz (Table 1), we infer that these compounds could also have an *antiperiplanar* conformation about the C–C–O–P bond. Further, similar ^{13}C chemical shifts (Table 2) observed for the choline part of these molecules suggest that the environment around the phosphocholine residue in all the three phospholipid species is similar. To determine the orientation of the phosphocholine head-group with respect to the glycerol/butanetriol backbone, we recorded the $^{1}H-^{1}H$ NOESY spectra (Fig. 4) of Ib, IIb and IIIb in $CDCl_3$ with a mixing time of 300 ms. These experiments indicate that in all the three compounds the time-averaged orientation of the head-group could be such wherein the choline methyl protons may lie within a 5 Å distance from the C2 methine proton of Ib (or IIIb) or the C3 methine proton of IIb.

To examine whether the above NMR spectral characteristics of II and III are retained even in their aqueous dispersions, we analysed the sonicated aqueous dispersions of Ib (T_m, 41.4°C), IIb (T_m, 35.1°C) or IIIb (T_m, 39.7°C) by both the ^{1}H- and ^{13}C-NMR spectroscopy at 50°C. Peak assignments were made by comparing the ^{1}H- and ^{13}C-NMR spectra of the various phospholipids in D_2O with that observed in $CDCl_3$. Although the ^{1}H-NMR spectra of all the three phospholipid molecular species in D_2O were similar to that in $CDCl_3$, it was not possible to calculate the coupling constants due to broadening of the proton peaks. However, the nonequivalence of the C2 methylene protons could still be clearly seen in the proton spectra of IIb (Fig. 5), suggesting that the butanetriol backbone conformation observed for II (or III) in $CDCl_3$ is largely retained even in the sonicated aqueous dispersions. This finds further support from our ^{13}C-NMR data (Table 2) which shows that the stereoelectronic environment of the glycerol/butanetriol backbone carbons did not significantly change by changing the dispersion medium. Whatever small differences (0.2–0.7 ppm) were seen in the chemical shifts of the various backbone carbon atoms upon moving from $CDCl_3$ to D_2O may be assigned to the differences in polarities of the two solvents, rather than to any alteration in the backbone conformation.

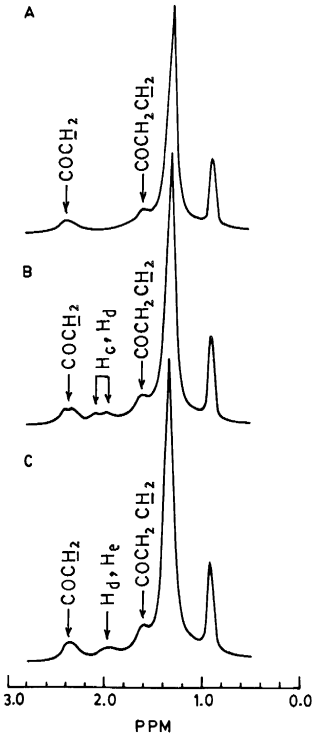

Fig. 5. 300 MHz ^{1}H-NMR spectra of sonicated aqueous dispersions (vesicles) of Ib (a), IIb (b), and IIIb (c). Only the hydrocarbon region has been shown to highlight the nonequivalent nature of the C2 methylene protons of the butanetriol backbone in II.

4. Discussion

This study indicates that the conformational preferences around the butanetriol C1–C2 bond in III or

C2–C3 bond in II could be similar to that around the glycerol C1–C2 bond in I. To further highlight the conformational preferences in the backbone region of the three phospholipids species, we utilized the three-staggered state conformational model representing the minimum free energy conformation. This model uses the vicinal proton–spin coupling constants, in each of the three possible conformations, as the component coupling constants [6,24] for determining the time-averaged distribution of the major conformational states. The values of the component coupling constants were taken from the literature [24,25]. Since the experimental spectra were successfully simulated using only one set of the vicinal coupling constants for each C–C or C–O bond, motional averaging between each of the three staggered conformations must occur that is fast on the NMR time scale. The fractional populations of three rotamers (Fig. 6) about each of the C–C bonds of glycerol and butanetriol backbones are summarized in Table 3. Since individually the geminal protons can not be assigned, two solutions are possible. For example, for a C–C bond with two protons, H_a and H_b, on one carbon and H_c on the second carbon, one set of solutions could be obtained by taking $J_{ac} < J_{bc}$, while the other set of solutions could be obtained by taking $J_{ac} > J_{bc}$, if H_a and H_b are chemically and magnetically nonequivalent.

As shown in Fig. 6 and Table 3, the two preferred conformations about the C1–C2 bond in Ib are the rotamer A characterized by the torsion angle θ_3/θ_4 = ap/sc and rotamer B with the torsion angle θ_3/θ_4 = sc/−sc. The conformation of rotamer A is the one that is found in majority of the single crystal structures of phospholipids [10]. Rotamer B is also represented in crystal structures, though to a lesser

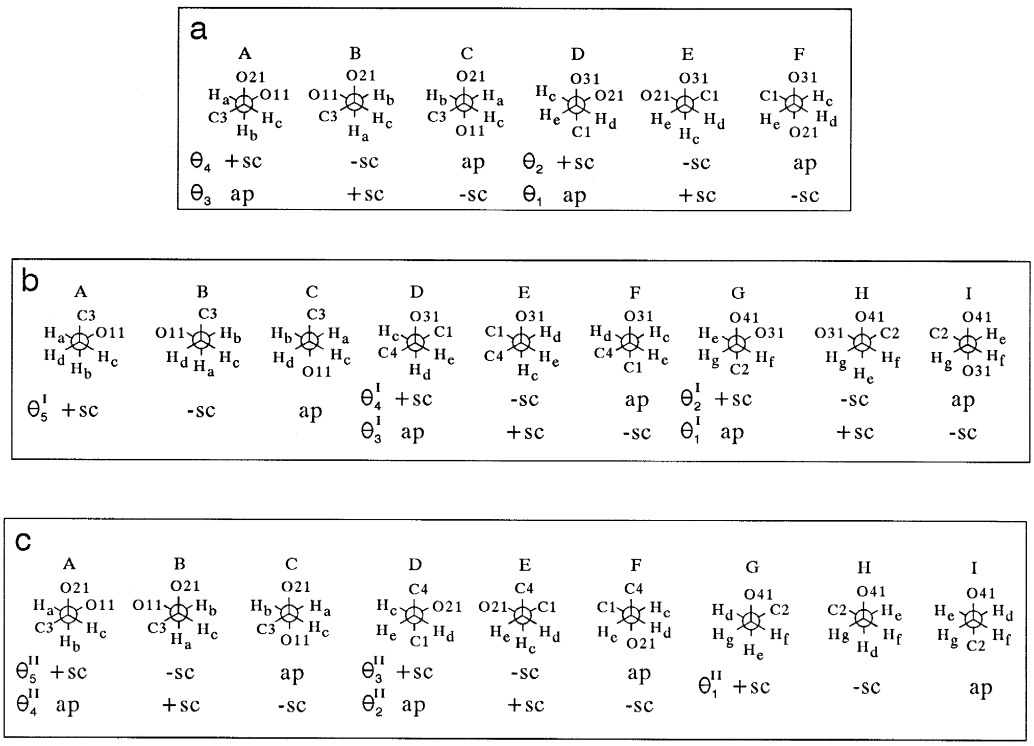

Fig. 6. Staggered conformations of minimum free energy about the C–C bonds of the glycerol/butanetriol backbone in Ib (a), IIb (b), and IIIb (c). (a) A–C, torsion angle θ_3 (O11–C1–C2–C3) and θ_4 (O11–C1–C2–O21) about the C1–C2 bond; D–F, torsion angle θ_1 (C1–C2–C3–O31) and θ_2 (O21–C2–C3–O31) about the C2–C3 bond. (b) A–C, torsion angle θ_5^{I} (O11–C1–C2–C3) about the C1–C2 bond; D–F, torsion angle θ_3^{I} (C1–C2–C3–C4) and θ_4^{I} (C1–C2–C3–O31) about the C2–C3 bond; G–I, torsion angle θ_1^{I} (C2–C3–C4–O41) and θ_2^{I} (O31–C3–C4–O41)about the C3–C4 bond. (c) A–C, torsion angle θ_4^{II} (O11–C1–C2–C3) and θ_5^{II} (O11–C1–C2–O21) about the C1–C2 bond; D–F, torsion angle θ_2^{II} (C1–C2–C3–C4) and θ_3^{II} (O21–C2–C3–C4) about the C2–C3 bond; G–I, torsion angle θ_1^{II} (C2–C3–C4–O41) about the C3–C4 bond. The terms sc and ap represent the *synclinal* and *antiperiplanar* conformation.

Table 3
Staggered-state rotameric distributions of minimum energy conformations in the glycerol/butanetriol backbone of Ib, IIb and IIIb

Molecular species	Rotamer population [a]								
	A	B	C	D	E	F	G	H	I
	$J_{ac} > J_{bc}(J_{ac} < J_{be})$ $J_{ac} > J_{ad}(J_{ac} < J_{ad})$ $J_{bc} > J_{bd}(J_{bc} < J_{bd})$			$J_{cd} > J_{ce}(J_{cd} < J_{ce})$ $J_{ce} > J_{de}(J_{cd} < J_{de})$			$J_{ef} > J_{eg}(J_{ef} < J_{eg})$ $J_{df} > J_{dg}(J_{df} < J_{dg})$		
Ib	56.29 (0.00)	38.70 (49.70)	5.00 (50.30)	37.62 (36.56)	30.12 (25.76)	32.26 (37.68)	–	–	–
	–	–	–	–	–	–	–	–	–
IIb	–	–	–	–	–	–	G + H = 79		21
	39.55 (37.49)	22.62 (31.00)	37.83 (31.51)	54.49 (0.00)	37.19 (49.51)	8.32 (50.49)	–	–	–
	26.74 (21.16)	48.08 (49.44)	25.18 (29.40)						
IIIb	54.40 (0.00)	42.48 (53.03)	3.12 (46.97)	32.95 (41.16)	43.97 (10.47)	23.08 (48.37)	5.87 (49.99)	43.66 (35.92)	50.47 (14.09)
	–	–	–	–	–	–	56.75 (59.44)	26.92 (15.80)	16.33 (24.76)
	–	–	–						

[a] Rotameric distributions (for nomenclature: see Fig. 6) were calculated from the observed vicinal spin coupling constants (see Table 1) as described in Section 2 and are expressed in percentages. For proton numbering: see Table 1.

extent. In monomeric solutions or micellar dispersions in which the phospholipid is in the liquid-crystalline form, rotamer A is also the dominant conformation [6]. Both rotamers A and B are *synclinal* (gauche) conformations, indicating that the two ester oxygen atoms linked to the glycerol C1 and C2 carbons have a *synclinal* (gauche) arrangement, i.e. $\theta_4 = +\text{sc}$ and $-\text{sc}$. In contrast, these oxygen atoms in rotamer C are *antiperiplanar*. This means that the two acyl chains in rotamers A and B could readily attain a parallel alignment, whereas such a stacking of these chains is difficult to achieve in rotamer C. Taking $J_{ac} > J_{bc}$, as has been conventionally done, gives a low value of conformer C and therefore this set of solution is more relevant to the conformational distribution, than by taking $J_{ac} < J_{bc}$, which gives a considerably high value of rotamer C. The 5% population observed by us for rotamer C by taking $J_{ac} > J_{bc}$ is quite close to the values reported earlier [6,7].

Similar analysis of IIIb about the C1–C2 bond, taking $J_{ac} > J_{bc}$, gives values (Table 3) which indicate a preference of the rotamers A and B over the rotamer C, suggesting that like Ib, the parallel alignment of the two hydrocarbon chains is preserved also in IIIb. Of the two solutions possible for the C2–C3 bond in IIIb, equal populations of the three conformers are obtained by taking $J_{cd} > J_{ce}$, which indicates a conformational flexibility in this region. However, for $J_{cd} < J_{ce}$, the rotamers D and F with $\theta_2^{II}/\theta_3^{II} = -\text{sc}/+\text{sc}$ and $+\text{sc}/\text{ap}$ respectively, are predominant. For the C3–C4 bond in IIIb, as there are two pairs of vicinally linked protons, there are four possible solutions to the conformational distribution. Irrespective of the choice of protons and coupling constants, conformation G is the preferred conformation with $\theta_1^{II} = +\text{sc}$ in three out of four solutions. These results clearly indicate that in spite of the presence of an additional methylene group (C3 methylene) between the two acyl chains and the phosphocholine moiety, which could be considered to impart flexibility to the methylene group bearing this choline moiety, as compared to Ib, there is a high degree of conformational preference about the C3–C4–O bond. This may be taken to suggest that the polar head-group in IIIb is perhaps much more ordered than in Ib. That this could indeed be the case is further supported by the results of our NOESY experiments where we have observed a stronger NOE peak between the *N*-methyl protons and the methine proton in case of IIIb, compared to Ib or IIb (Fig. 4).

Out of the two butanetriol-based phospholipids, IIb is closer to LPPC [23], rather than Ib, in terms of its conformational preferences. As the C1 and C2 carbon atoms in IIb are attached with two protons each, four solutions are possible to the conformational distribution about the C1–C2 bond. However, only a slight preference for a single conformer B with $\theta_5^{I} = -\text{sc}$ could be observed by taking $J_{bc} > J_{bd}$ (or $J_{bc} < J_{bd}$) (Table 3), indicating that this region of the phospholipid molecule has a considerable degree of flexibility, with the primary acyl chain independent to move with respect to the interface. Also, it suggests that the C=O group of the C1 ester moiety has a freedom to orient itself with respect to the rest of the molecule. For the C2–C3 bond, the two solutions obtained ($J_{cd} > J_{ce}$ and $J_{cd} < J_{ce}$) resemble somewhat those obtained for the C1–C2 bond of the glycerol backbone in Ib or the butanetriol backbone in IIIb, although no acyl chain is linked with this methylene residue in IIb. These results clearly indicate that structurally the C2 methylene residue in IIb represents the proximal beginning of the primary acyl chain. Also, it suggests that the intramolecular acyl chain interaction is the primary factor that determines the preferred conformation of the glycerol C1–C2 bond, and that to have an effective interaction, a vicinal arrangement of the interacting chains is required. For the C3–C4 bond in IIb there is no conformational preference with $\pm\text{sc} = 79\%$ and ap $= 21\%$ (in close similarity to LPPC structure [23] in terms of chemical shift and magnetic equivalence), and therefore, there are no restraints to the free rotation around the C3–C4 bond of the butanetriol backbone in IIb.

These results demonstrate that an insertion of one additional methylene residue between the glycerol C2 and C3 carbon atoms in I does not appreciably affect the conformational preference around the C1–C2 bond. However, no conformational preference is observed around this bond if the additional methylene is introduced between the glycerol C1 and C2 carbon atoms. In this case, the preferred conformation of the resulting PC analog (compound II) is such wherein the additional methylene, rather than the C1 methylene, serves as the proximal beginning of the primary acyl chain. From these results, we conclude that the

glycerol backbone conformation in phosphatidylcholines is governed primarily by the intramolecular acyl chain interactions which essentially require a vicinal arrangement of the two acyl chains in phospholipid molecule.

Acknowledgements

We thank Professors G. Govil and R.V. Hosur (TIFR, Bombay) for providing us the 500 MHz NMR facility and also for their help in computer simulations of the experimental spectra. Also, we gratefully acknowledge the help of Dr. A.K. Bhatnagar (IOC, Faridabad) for granting us permission to use his 300 MHz NMR facility.

References

[1] Hauser, H. and Poupart, G. (1991) in The Structure of Biological Membranes (Yeagle, P., ed.), pp. 3–71, CRC Press, Boca Raton, FL.
[2] Gennis, R.B. (1989) Biomembranes: Molecular Structure and Function, Chap. 2, pp. 36–84, Springer, New York.
[3] Seelig, J. (1977) Q. Rev. Biophys. 10, 353–418.
[4] Seelig, J. and Seelig, A. (1980) Q. Rev. Biophys. 13, 19–61.
[5] Hauser, H., Pascher, I., Pearson, R.H. and Sundell, S. (1981) Biochim. Biophys. Acta 650, 21–51.
[6] Hauser, H., Pascher, I. and Sundell, S. (1988) Biochemistry, 27, 9166–9176.
[7] Han, X., Chen, X. and Gross, R.W. (1991) J. Am. Chem. Soc. 113, 7104–7109.
[8] Smith, S.O., Hamilton, J., Salmon, A. and Bormann, B.J. (1994) Biochemistry 33, 6327–6333.
[9] Hübner, W., Mantsch, H.H., Paltauf, F. and Hauser, H. (1994) Biochemistry 33, 320–326.
[10] Pascher, I., Lundmark, M., Nyholm, P.-G. and Sundell, S. (1992) Biochim. Biophys. Acta 1113, 339–373.
[11] Lucas, H.J., Mitchell, F.W., Jr. and Scully, C.N. (1950) J. Am. Chem. Soc. 72, 5491–5497.
[12] Edmundson, R.S. (1962) Chem. Ind. (London) 1828–1829.
[13] Hernandez. O., Chaudhary, S.K., Cox, R.H. and Porter, J. (1981) Tetrahedron Lett. 22, 1491–1494.
[14] Goswami, S.K. and Frey, C.F. (1971) J. Lipid Res. 12, 509–510.
[15] Cevc, G. (1992) in Hydration of Macromolecules (Westhof, E., ed.), pp. 338–390, Macmillan, New York.
[16] Dervichian, O.G. (1964) Prog. Biophys. Mol. Biol. 14, 263–342.
[17] Haasnoot, C.A.G., De Leeuw, F.A.A.M. and Altona, C. (1980) Tetrahedron 36, 2783–2792.
[18] Colucci, W.J., Jungk, S.J. and Gandour, R.D. (1985) Magn. Reson. Chem. 23, 335–343.
[19] Bhakuni, V. and Gupta, C.M. (1989) Biochim. Biophys. Acta 982, 216–222.
[20] Gupta C.M., Radhakrishnan, R. and Khorana, H.G. (1977) Proc. Natl. Acad. Sci. USA 74, 4315–4319.
[21] Agarwal, K., Bali, A. and Gupta, C.M. (1984) Chem. Phys. Lipids 36, 169–178.
[22] Chandrakumar, N.S. and Hajdu, J. (1982) Tetrahedron Lett. 23, 1043–1046.
[23] Hauser, H., Guyer, W., Spiess, M., Pascher, I. and Sundell, S. (1980) J. Mol. Biol. 137, 265–282.
[24] Hauser, H., Guyer, W., Spiess, M., Pascher, I., Skrabal, P. and Sundell, S. (1980) Biochemistry 19, 366–373.
[25] Abraham, R.J. and Gatti, G. (1969) J. Chem. Soc. B, 961–968.